Sains Malaysiana 51(7)(2022): 2119-2128
http://doi.org/10.17576/jsm-2022-5107-14

Optimization and Characterization of Fatty Acid Esters (FAES) Based Nanostructured Lipid Carrier (NLC) by Box-Behnken Analysis

(Pengoptimuman dan Pencirian Ester Asid Lemak (FAES) Berasaskan Pembawa Lipid Berstruktur Nano (NLC) oleh Analisis Box-Behnken)

SARAH SHAZWANI S. & MISNI MISRAN*

Department of Chemistry, Faculty of Science, University of Malaya, 50603 Kuala Lumpur, Federal Territory, Malaysia

Received: 29 August 2021/Accepted: 30 December 2021

ABSTRACT

An unfavorable rate of toxicity and hydrophobicity of active substance in water has prompted the development of an improved active ingredients delivery systems such as nanostructured lipid carriers (NLC). This present study investigates varying components of NLCs compositions to achieve an optimized and stable colloidal suspension of NLCs through Box-Behnken design analysis for potential use as an active substance carrier system. The optimised formulation is comprised of 2.9% stearic acid, 0.4% MCT, 0.3% IPM, 0.37% Tween 20, 0.23% Span 20 and 96% deionised water (DW). The mean particle size, polydispersity index, and zeta potential of the optimized NLCs were 322±13.5 nm, 0.199±0.04, and -36±0.1 mV, respectively. Based on the TEM micrograph, NLCs can be observed as having an elongated spherical shape with a dense appearance.

Keywords: Box-Behnken design; isopropyl myristate; medium-chain triglyceride; nanostructured lipid carrier; surfactant

ABSTRAK

Tahap ketoksikan dan sifat hidrofobik sesetengah bahan aktif yang kurang memberangsangkan telah mendorong kepada kajian berkenaan sistem penyampaian ubat yang lebih baik seperti pembawa lipid berstruktur nano (NLC). Justeru, penyelidikan ini mengkaji potensi NLC sebagai sistem pembawa ubat yang baik melalui penelitian kepelbagaian komponen komposisi NLC untuk mencapai suspensi koloid yang stabil dan optimum melalui analisis reka bentuk Box-Behnken. Formulasi yang dioptimumkan terdiri daripada 2.9% asid stearat, 0.4% MCT, 0.3% IPM, 0.37% Tween 20, 0.23% Span 20 dan 96% air deionisasi (DW). Saiz zarah min, indeks polidispersi dan potensi zeta NLC yang optimum masing-masing adalah 322±13.5 nm, 0.199±0.04 dan -36±0.1 mV. Berdasarkan mikrograf TEM, NLC dapat dilihat memiliki bentuk sfera memanjang dengan penampilan yang padat.

Kata kunci: Isopropil miristat; pembawa lipid berstruktur nano; reka bentuk Box-Behnken; surfaktan; trigliserida rantai sederhana (MCT)

INTRODUCTION

Conventional drug delivery system has always been associated with various issues such as poor solubility, poor drug delivery, insufficient bioavailability, and high toxicity which leads to the developments of self-assembled colloidal lipid systems such as solid lipid nanoparticles (SLN), and nanostructured lipid carriers (NLCs). Nanostructured lipid carriers (NLCs) are drug-delivery systems derived from the 1st generation of solid lipid nanoparticles (SLN) which are composed of both solid and liquid lipids as a core matrix. It was shown that NLCs show some advantages for drug therapy over conventional carriers, including increased solubility, the ability to enhance storage stability, improved permeability and bioavailability, reduced adverse effect, prolonged half-life, and tissue-targeted delivery (Gordillo-Galeano & Mora-Huertas 2018: Sakamula et al. 2021). In contrast to the highly ordered solid lipid nanoparticle (SLN) being yielded from solid lipids or blends of solid lipids, the incorporation of liquid lipids to solid lipids leads to massive crystal order disturbance (Mishra et al. 2018).

The resulting matrix of lipid particles shows great imperfections in the crystal lattice and leaves enough space to accommodate drug molecules, thus, leading to improved drug loading capacity (Shirodkar et al. 2019). The small size of lipid particles ensures close contact to the stratum corneum and can enhance drug flux through the skin, and due to their solid lipid matrix, a controlled release from these carriers is possible (Khezri et al. 2018). The extend of NLCs stability is highly dependent on its makeup components. Hence, it is essential to understand the colloidal nature and behaviour of the active ingredient, as well as their compatibility with the NLCs make up ingredients, as it can provide better insight into the system as an active ingredient delivery carrier (Yew & Misran 2019). Accordingly, this present study aimed towards the development of optimized and efficacious NLCs through an investigation of suitable and appropriate compositions of lipids and surfactants by Box-Behnken Design analysis without compromising its safety.

Materials and Methods

MATERIALS

Stearic acid, Isopropyl myristate, Tween 20, Tween 60, Tween 80, Span 20, Span 60, Span 80 and PBS (phosphate-buffered saline) tablets were purchased from Sigma Aldrich (St. Louis, USA). Medium-chain triglycerides (MCT) and virgin coconut oil (VCO) were purchased from a local pharmacy (Caring Pharmacy, Malaysia). Glyceryl monostearate and oleic acid were obtained from Merck. Box-Behnken Analysis tools were purchased from NCSS2020 statistical software (2020), NCSS, LLC. All solutions and samples were prepared by using deionized water with the resistivity of 18.2 Ωcm-1, which was supplied from a Barnstead Diamond Nanopure Water Purification unit coupled with a Barnstead Diamond RO unit (Barnstead International, USA).

LIPID SCREENING

Lipid screening was implemented to determine the suitability of the lipids including the solubility and miscibility of the active ingredient with the selected lipids. For solid lipids, a mixture of solid lipid and liquid lipid were heated at 5-10 °C above its melting point. As for the liquid lipid, 0.05 g of Quercetin was dissolved in 2 mL of each material. The mixtures were further subjected to vortex mixing followed by orbital shaking at 37±1.0 °C for 48 h. The equilibrated samples were centrifuged at 3000 rpm; the supernatant was filtered, and the filtrates were diluted with the appropriate solvent. The solubility of Quercetin was measured at 379 nm by using the validated UV spectrophotometric method. All estimations were done in triplicates (Ni et al. 2014).

THERMAL BEHAVIOR NLCS AND THEIR RAW MATERIALS

The thermal behaviour of NLCs and their components were expressed using Differential Scanning Calorimetry (DSC). Sample of approximately 2-3 mg was weighted in an aluminium hematic pan of 40 µL capacity and the thermal curve were obtained by performing DSC analysis with temperature ranging from 20 to 100 °C at a scan rate of 5 °C per min. The analysis was conducted thrice, and an empty aluminium pan was used for reference. Data were analyzed using the software TA Instruments Universal Analysis 2000, 4.7A. Thermal transitions of NLCs and their binary component were visualized separately using hot-stage microscopy (HSPOM).

HOT-HOMOGENIZATION METHOD

NLCs were prepared by using the hot-homogenization technique using a high shear homogenizer. The lipid phase was heated in a water bath at 80 °C until the mixture becomes a clear liquid under constant stirring. Simultaneously, a pre-heated surfactant solution of similar temperature was dispersed into the molten lipid phase and homogenized under strong agitation of 18,000 rpm (T25 basic homogenizer IKA, Germany). The hot emulsion was then rapidly poured into the cold water of approximately 2 °C under magnetic stirring, where solidification of lipids and formation of NLCs was completed (Eh Suk et al. 2020).

BOX-BEHNKEN ANALYSIS FOR OPTIMIZATION OF NLCS

Optimization of NLCs formulation was achieved using 'Box-Behnken design (BBD)' (NCSS2020 statistical software). The subsequent effect of relative correlations between independent variables on selected dependent variables was further validated using multiple regression analysis (NCSS2020), in which a suitable quadratic model was generated (Table 1). Restrictions were imposed on each selected parameter that could impact the characteristics of the formulation.

TABLE 1. Selected independent variables and their analysis coding used in BBD for the formulation of NLCs

Factors/Variables	Low (-1)	Medium (0)	High (+1)
Independent variables			
A = MCT oil (%)	0%	0.2%	0.6%
B = Surfactant (%)	2%	2.5%	3%
C = Homogenization period (min)	6 min	8 min	10 min

STABILITY OBSERVATION OF OPTIMIZED NLC

To determine the effect of storage on the average particle size, polydispersity index, and zeta potential of the formulation, a stability analysis was implemented. The estimation of these parameters was carried out in triplicate. The formulations were placed in an airtight container and stored at room temperature (27 °C) for 28 days. Particle sizes, polydispersity index (PDI), and zeta potential of each NLCs formulation were measured using Malvern Nano series Zetasiser (Malvern Instrument, UK) at 27 °C with a backscattering angle of 173°. Approximately 50 µL of NLCs were diluted in 5 mL deionized water filtered using 0.45 µL PTFE membrane filter prior to measurement to ensure the absence of external debris and dust. Preparation of a highly disperse and almost clear system is imperative to the mechanism of the dynamic light scattering technique used by the Malvern Nano series Zetasiser. A system with high viscosity would cause a false interpretation of multiple scattering of light scattered by only one particle due to the close distance between one particle and another. Each measurement was conducted three times to ensure the certainty of the result.

MORPHOLOGY AND SURFACE CONDITION OF THE NLCS

The surface morphology of NLCs also was visualized under TEM (Carl Zeiss Libra®, 120). Approximately 3 drops of NLC solution were deposited onto a 400-mesh copper grid and were left in ambient for 3 min. The excess solution was removed by carefully blotting it onto filter paper. Two drops of 3% Phosphotungstic acid stain were placed onto the grid and left to air-dry at room temperature before TEM observation.

RESULTS AND DISCUSSION

LIPID SCREENING AND SELECTION OF SURFACTANT

The solubility of the standard, Quercetin was found to be less in stearic acid than in Glyceryl monostearate (GMS) as shown in Table 2. In addition to that, an increased pattern of quercetin solubility in liquid lipids can be seen in the following order; oleic acid, virgin coconut oil, MCT, and isopropyl myristate. Despite GMS having the highest solubility of Quercetin, it is deemed unsuitable to be used as solid lipid in the system due to its low melting point hence, stearic acid was selected as the suitable solid lipid for the formulation while Isopropyl myristate was chosen as its liquid lipid counterpart. However, since IPM generally has a low viscosity of 6 mPa.s at 20 °C, a concern pertaining to its ability in disrupting the ordered crystalline structure of the matrix core was addressed. Thus, the incorporation and synergistic alliance of IPM and MCT with slightly higher viscosity values were investigated.

Different non-ionic surfactants mixtures were selected for surfactant screening before NLCs formulation due to their ability to minimize particle size increment and the tendency of particle aggregation (Subramaniam et al. 2020). NLCs with incorporated Tween 20/Span 20 (TS20), Tween 60/Span 60 (TS60), and Tween 80/Span 80 (TS80) were formulated and monitored for size increments and PDI for 28 days (Figure 1). Synergistic application of multiple surfactants in a system has been documented to lowers the PDI and further inhibit aggregation of particles (Severino et al. 2011).

Particle size measurements of TS20, TS60, TS80 were 294.833 nm, 265.766 nm, and 364.8 nm on the first day with total increments of 6.41, 15.24, 34.56%, respectively, over the subsequent 28 days. Higher particle size of TS80 is attributable to the presence of bend and kink at the double bond of monooleate in Tween 80, which increases the curvature of the NLC particles (Teo et al. 2011). The gradual particle size increase from TS20 to TS60 and TS80 was highly likely due to the polymeric chain of each respective surfactant

which contingently instigate the flocculation of particles through their strong van der Waals interactions (Eh Suk et al. 2020).

An investigation by Kothekar had reported poorer emulsifying power of tween 60 and tween 80 compared to tween 20 due to the lacking of adsorption ability at the interface and thus leading to higher interfacial energy, inducing instability of the system (Kothekar et al. 2007). On the 14th day, half mark of the formulation's physical observation, slight flocculation of the formulation was seen in TS60 and TS80 which explains sudden instability in size and PDI measurements. However, the PDI of all three formulations was below 0.5, indicating a uniform distribution of the dispersion.

TABLE 2. Solid and liquid lipid screening prior to NLC development

Liquid lipid	QUE solubility (mg/mL)	QUE solubility, %
Oleic acid	2.6±0.04	13%
MCT oil	3±0.02	15%
Virgin coconut oil	2.8±0.02	14%
Isopropyl myristate	3.2±0.06	16%
Solid lipid	QUE solubility (mg QUE/g)	
Stearic acid	2.5±0.01	
Glyceryl monostearate (GMS)	3±0.03	

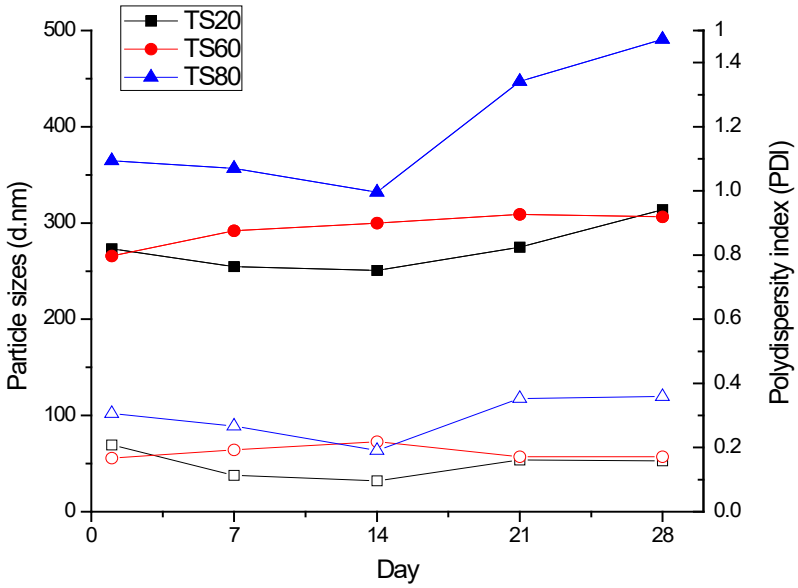

FIGURE 1. Mean particle size (solid symbol) and polydispersity index (open symbol) of TS20 (■), TS60 (●), TS80 (▲), as a function of the storage period, at 25 °C

THERMAL BEHAVIOR NLCS AND THEIR RAW MATERIALS

Pure stearic acid, lipid phase mixture, and blank NLCs were subjected to DSC analysis to determine changes in heat flow caused by any physicochemical changes with the system with respect to temperature and time. The DSC thermograms of stearic acid and lipid phase mixture are shown in Figure 2. Stearic acid as a solid lipid performed an onset temperature at 69.5 °C and a peak temperature point at 72.5 °C which indicated the crystalline transition of solid-to-liquid. The lipid phase mixture presented onset temperature and melting peak of 64.2 °C and 67.4 °C, respectively, which is slightly lower than bulk stearic acid suggesting the formation of amorphous structure, thus allowing better encapsulation of drug (Figure 3). A similar condition can be seen in the thermograms measurement of the blank NLC, inferring the loss in the crystallinity of stearic acid (Table 3).

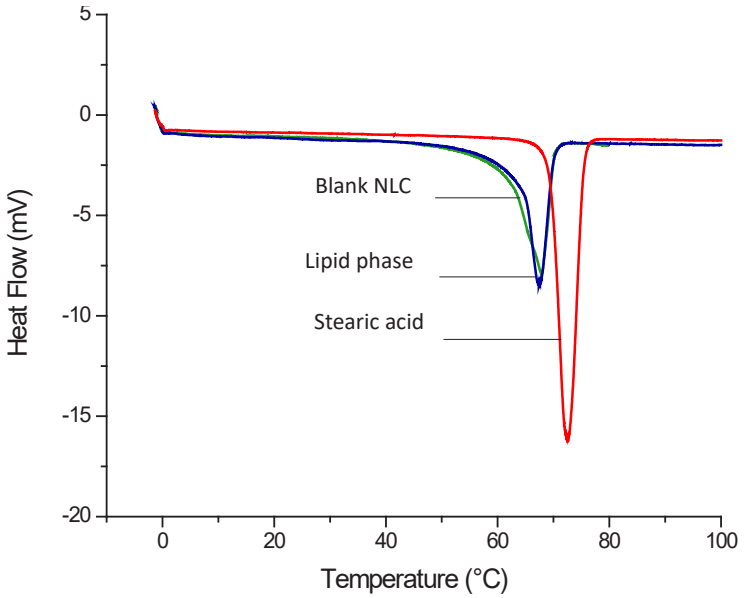

FIGURE 2. Differential scanning calorimetry thermogram of NLC. The experiment was performed from 25 to 100 °C at a scan rate of 5 °C per min

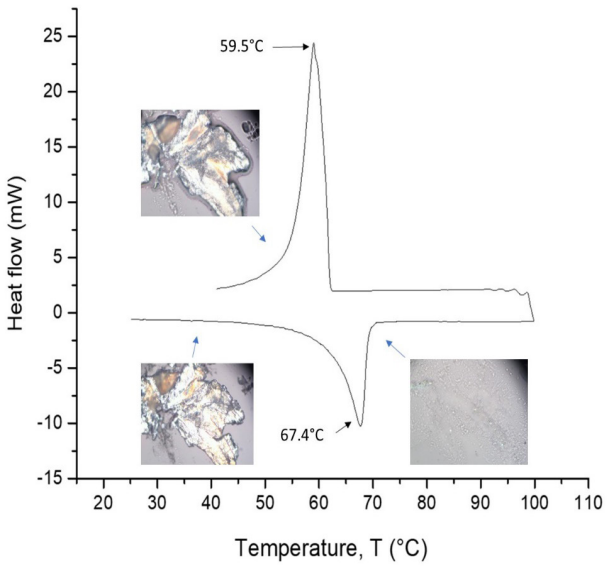

FIGURE 3. HSPOM micrographs of blank NLC corresponding to complete melting and crystallization process at each respective onset temperature to 27 °C (room temperature)

TABLE 3. Thermal parameter of stearic acid, lipid phase mixture and blank NLC

	Onset temperature, (°C)	Peak temperature, (°C)	Melting enthalpy, ΔH (J g-1)
Stearic acid	69.5	72.5	180.0
Lipid phase	64.2	67.4	137.6
Blank NLC	61.5	67.4	134.0

OPTIMIZATION OF FORMULATION USING BOX-BEHNKEN DESIGN ANALYSIS (BBD)

Optimization of the formulations was achieved by the means of 'Box-Behnken design (BBD)' comprises of three factors at three varying levels. Direct correlation of the selected independent variables i.e., the concentration of MCT (F^1), the concentration of surfactant (F^2), homogenization period (F^3) on the dependent variables i.e., particle size (A), polydispersity index (PDI) (B), and zeta potential (C) was investigated and depicted as 3-D surface plots in Figure 4.

Table 4 showcase the observed results of 15 generated formulations while summary response of the dependent variables by regression analysis and the resulting quadratic model were shown in Table 5.

TABLE 4. Observed responses in BBD design for optimization of NLCs

Formulation labels	Independent variables			Dependent variables		
	F^1	F^2	F^3	A	B	C
SR1	0	2.5	6	564.7±4.97	0.433±0.003	-36.5±0.8
SR2	0.2	2	8	426.9±3.97	0.316±0.04	-35.8±0.3
SR3	0.6	2.5	8	426.2±4.65	0.299±0.02	-36±0.10
SR4	0	3	6	559.7±1.06	0.446±0.004	-36.7±0.3
SR5	0.6	2.5	10	338.2±2.21	0.219±0.02	-35.1±0.23
SR6	0.6	3	6	511.4±1.27	0.351±0.01	-36.6±0.6
SR7	0.6	2	8	415.1±3.11	0.286±0.01	-35.7±0.09
SR8	0.6	2	10	294.3±7.08	0.230±0.01	-35±0.1
SR9	0.2	2	10	383±4.60	0.237±0.04	-35.3±0.32
SR10	0.2	2.5	10	370.2±10.0	0.25±0.02	-35.5±0.09
SR11	0.2	3	8	492±4.63	0.342±0.06	-36.1±0.45
SR12	0	2.5	6	554.8±2.09	0.433±0.03	-36.5±0.28
SR13	0	3	6	552.2±2.23	0.446±0.01	-36.7±0.5
SR14	0.2	2	10	376.3±4.05	0.237±0.02	-35.3±0.12
SR15	0	2	6	535.3±2.33	0.405±0.07	-36.3±0.22

TABLE 5. Summary results of Multiple regression analysis for response R^1, R^2, R^3 for resulted quadratic model

Quadratic model	R^2	Adjusted R^2	SD	P-value	%CV
Particle size (nm) (R^1)	0.994	0.983	92.7	0.019	0.026
Polydispersity index (PDI) (R^2)	0.998	0.995	0.090	0.031	0.018
Zeta potential (mV) (R^3)	0.990	0.972	0.563	0.027	-0.002

Regression equation for fitted quadratic model

Particle size (nm) (R1) 1174.95605381118 + 10.1281763821587 × F1 + 12.2035874439292 × F2 - 152.884865470721 × F3 - 390.708146486877 × F1 × F1 - 21.4999999999169 × F1 × F2 + 35.2197309417027 × F1 × F3 - 25.2816143497622 × F2 × F2 + 21.9820627802607 × F2 × F3 + 2.65241031389505 × F3 × F3

Polydispersity index (PDI) (R2) -0.192678090966499 - 0.422218663249347 × F1 + 0.194603459320907 × F2 + 0.106126201152905 × F3 + 0.524778453981802 × F1 × F1 + 0.00714285714274568 × F1 × F2 - 0.0117881165919187 × F1 × F3 - 0.0260858424087207 × F2 × F2 - 0.00444586803329892 × F2 × F3 - 0.00744722934015704 × F3 × F3

Zeta potential (mV) (R3) -32.0108263933442 + 4.91848174246668 × F1 - 1.01223574631642 × F2 - 0.830637411913753 × F3 - 4.98798846892419× F1 × F1 - 0.857142857141892 × F1 × F2 + 0.125560538116505 × F1 × F3 + 0.0962203715568132 × F2 × F2 + 0.0326073030107876 × F2 × F3 + 0.0531630365149746 × F3 × F3

PARTICLE SIZE (A)

The coefficient of determination (R^2) for A response relative to the independent variables was 0.994, with an adjusted R^2 of 0.983, indicating a well proportionate fit. Statistical evaluations by ANOVA showed a significant model term with a p-value < 0.050. By referring to the plotted 3-D surface figure (Figure 4(A)), a consistent pattern of reduced particle size of formulations was observed with the increasing concentration of MCT. The addition of MCT in the formulation compromised the viscosity of the lipid phase, and thus, forming smaller-sized particles due to reduced surface tension (Zhang et al. 2020).

On a contrary, the particle size of NLCs increased with the increasing concentration of surfactant incorporated. This is attributable to excess usage of surfactants relative to the lipid phase leading to subsequent bigger-sized NLCs. A previous investigation had shown that elevating the concentration of surfactant decreases the particle size due to reduction in interfacial tension among the lipids and the surrounding medium, hence causes partition of particles (Bnyan et al. 2018). However, there is a limit as to how much surfactants used can actually benefit the system. Excess incorporation of surfactants would result in aggregations of particles and an increase in size (Sarheed et al. 2020). The homogenization period also heavily affects the particle size as smaller-sized NLCs can be seen with a longer homogenization period. Overall, among the 15 experimented formulations, SR8 presented the least particle size of 280.9 nm, with SR1 offering a maximum particle size of 564.7 nm.

POLYDISPERSITY INDEX (PDI) (B)

The coefficient of determination (R^2) of the PDI with independent variables was 0.998, with an adjusted R^2 of 0.995, and a p-value of 0.011 implying a good model fit. Visualization of the effect of the independent variables on the PDI can be seen in the 3D surface plot, Figure 4(B), PDI values of the formulations correspond with its particle size, in which larger-sized particles often time have greater PDI and vice versa (Kaur et al. 2016). Despite that, to a certain extent, an increase in surfactant content in the formulation could induce aggregation of the particle due to bimodal distribution leading to populations with varied sizes (Sarheed et al. 2020). An experiment conducted by Ferreira et al. (2007) presented increased PDI of Methotrexate-loaded NLCs with raised PVA concentration. In contrast, increments

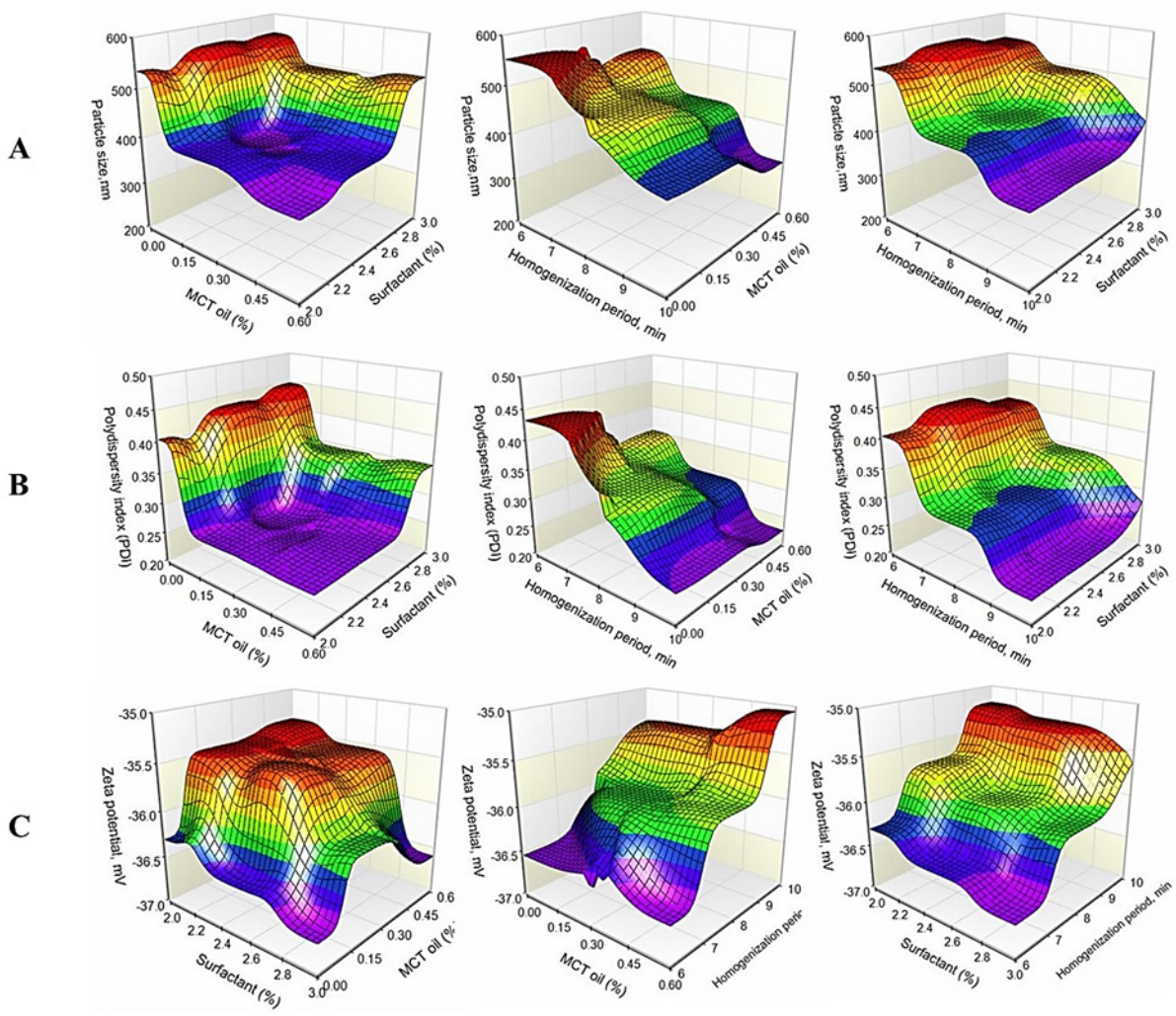

FIGURE 4. 3D-response surface plot showing the effect of independent variables on particle size (A), polydispersity index (B), and zeta potential (C)

of MCT and homogenization speed used during the formulation results in decreased PDI. Overall, PDI of the formulated NLCs ranges from 0.186 up until 0.446 which suggests homogenous distribution within the formulation (Dudhipala & Gorre 2020).

ZETA POTENTIAL (C)

The coefficient of determination (R^2) of zeta potential with independent variables was 0.990, with an adjusted R^2 of 0.972, and p-value of <0.05, suggesting a good model fit. The zeta potential of 15 generated formulations was evaluated to predict the long-term physical stability of the NLCs. As shown in Figure 4(C), no sign of trend was discovered with increments of MCT introduced to the system, as documented by Gardouh et al. (2018) in their study. It is also depicted in the figure that increasing surfactant concentration leads to a slight increase value of zeta potential, indicating the physical stability of the system through steric stabilization (Han et al. 2008). Homogenization speed was shown to have an insignificant effect on zeta potential with the highest and lowest value being -36.7 and -35 mV, respectively. All of the experimented formulations possess zeta potential values of more than -30 mV which generally signify the long-term stability of the system as mentioned by Muller in 2002 (Müller et al. 2002).

STABILITY STUDIES

Following the experimental analysis of the 15 generated formulations, NLC formulation that exhibit the smallest

size, lowest PDI, and appropriate zeta potential were further monitored for 28 continuous days to ensure the stability of the system over a long-term storing period. SR8 has shown particle size of 294.83 nm on day 1 of storing and only depicted slight increments of 9.36% of the initial size throughout the 28 days with no observable sign of sample instability at room temperature and at 4 °C, suggesting stable formulation. Consistent PDI measurement value of below 0.2 further suggesting homogeneous dispersion of particles.

The highest selected concentration of MCT in the lipid phase was incorporated in SR8 formulation with surfactant tween 20 and span 20 concentrations of 2%- and 10-min homogenization period. Liquid lipid lowers the melting temperature of lipid nanoparticles in accordance with the imperfection. Even then, due to the temperature factor, the amount of liquid lipid that can be added into the NLC is still limited which address the importance of NLC retaining its solid particle at least at body temperature of 37 °C; to disregard the possibility of it being an oil-in-water dispersion (Souto & Müller 2006; Vieira et al. 2020).

According to Yew and Misran (2019), incorporation of liquid lipid any higher than 30% of the lipid components was deemed unsuitable as an oil droplet detached from the NLC might be formed. SR8 was formulated using 20% of liquid lipid relative to the total lipid phase with 42% of it comprised of MCT and the rest of IPM. Over the course of storage, the formulation shows no physical changes and remained homogeneous (Figure 5).

Visual observation of SR8 after 28 days of monitoring was observed using transmission electron microscopy (TEM). The TEM micrograph of SR8 exhibits the absence of separated oil droplet formation and elongated shape of particles due to a high content of liquid lipid; causing disoriented matrix structure, hence prevented rigid rounded shape (Yew & Misran 2019). High-pressure homogenization of NLCs might also result in the occurrence of shear stress which consequently causes the stretching of the particles and thus, the elongated shape.

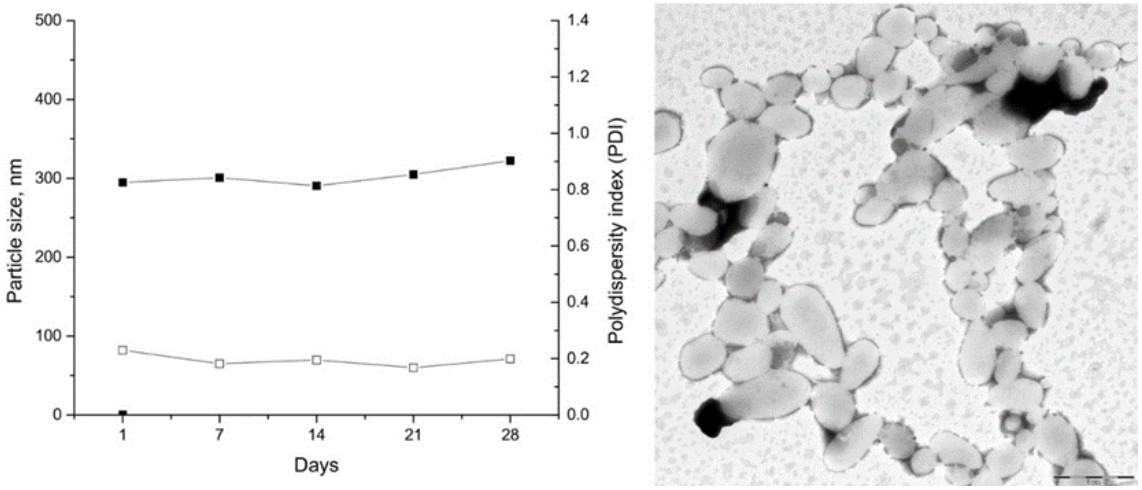

FIGURE 5. Particle size (solid symbol) and polydispersity index (open symbol) of SR8 (left), and TEM micrograph of SR8 (right) taken at 10,000 × magnification using Carl Zeiss LIBRA® 120

CONCLUSION

This current work investigates the development of an optimized nanostructured lipid carrier (NLC) system by Box-Behnken Analysis. Using BBD, 15 random formulations were generated and experimented with. An optimized formulation was successfully prepared by incorporation of 0.6% MCT in the lipid mixture, 2% of surfactant mixture, and 10 min homogenization period at 18,000 rpm speed. An appropriate and balanced composition of lipids and surfactants in the formulation resulted in an optimized NLC with a mean particle size of 322±13.5 nm and no sign of instability for over 28 days of observation. Elongated shaped particles can be observed in the TEM micrograph of the optimized NLC. Although organoleptic evaluation of the optimized NLC did not show any sign of formulation instability, further extensive stability studies might need to be carried out for an extended period.

ACKNOWLEDGEMENTS

The authors would like to express gratitude to Universiti Malaya (FP075-2018A) and the Ministry of Higher Education, Malaysia (FRGS/1/2018/STG07/UM/01/1) for giving us the chance to work on this study.

REFERENCES

Bnyan, R., Khan, I., Ehtezazi, T., Saleem, I., Gordon, S., O'Neill, F. & Roberts, M. 2018. Surfactant effects on lipid-based vesicles properties. *Journal of Pharmaceutical Sciences* 107(5): 1237-1246.

Dudhipala, N. & Gorre, T. 2020. Neuroprotective effect of ropinirole lipid nanoparticles enriched hydrogel for parkinson's disease: *In vitro, ex vivo,* pharmacokinetic and pharmacodynamic evaluation. *Pharmaceutics* 12(5): 448.

Eh Suk, V.R., Latif, F.M., Teo, Y.Y. & Misran, M. 2020. Development of nanostructured lipid carrier (NLC) assisted with polysorbate nonionic surfactants as a carrier for L -ascorbic acid and Gold Tri.E 30. *Journal of Food Science and Technology* 57(9): 3259-3266.

Ferreira, S.C., Bruns, R.E., Ferreira, H.S., Matos, G.D., David, J.M., Brandão, G.C., da Silva, E.P., Portugal, L.A., Dos Reis, P.S., Souza, A.S. & Dos Santos, W.N.L. 2007. Box-Behnken design: An alternative for the optimization of analytical methods. *Analytica Chimica Acta* 597(2): 179-186.

Gardouh, A.R., Faheim, S.H., Noah, A.T. & Ghorab, M.M. 2018. Influence of formulation factors on the size of nanostructured lipid carriers and nanoemulsions prepared by high shear homogenization. *International Journal of Pharmacy and Pharmaceutical Sciences* 10(4): 61-75.

Gordillo-Galeano, A. & Mora-Huertas, C.E. 2018. Solid lipid nano-particles and nanostructured lipid carriers: A review emphasizing on particle structure and drug release. *Eur. J. Pharm. Biopharm*. 133: 285-308.

Han, F., Li, S., Yin, R., Liu, H. & Xu, L. 2008. Effect of surfactants on the formation and characterization of a new type of colloidal drug delivery system: Nanostructured lipid carriers. *Colloids and Surfaces A: Physicochemical and Engineering Aspects* 315(1-3): 210-216.

Kaur, P., Garg, T., Rath, G., Murthy, R.S.R. & Goyal, A.K. 2016. Development, optimization and evaluation of surfactant-based pulmonary nanolipid carrier system of paclitaxel for the management of drug resistance lung cancer using Box-Behnken. *Drug Delivery* 23(6): 1912-1925.

Khezri, K., Saeedi, M. & Dizaj, S.M. 2018. Application of nanoparticles in percutaneous delivery of active ingredients in cosmetic preparations. *Biomedicine & Pharmacotherapy* 106: 1499-1505.

Kothekar, S.C., Ware, A.M., Waghmare, J.T. & Momin, S.A. 2007. Comparative analysis of the properties of Tween-20, Tween-60, Tween-80, Arlacel-60, and Arlacel-80. *Journal of Dispersion Science and Technology* 28(3): 477-484.

Mishra, D.K., Shandilya, R. & Mishra, P.K. 2018. Lipid based nanocarriers: A translational perspective. Nanomedicine: *Nanotechnology, Biology and Medicine* 14(7): 2023-2050

Müller, R.H., Radtke, M. & Wissing, S.A. 2002. Solid lipid nanoparticles (SLN) and nanostructured lipid carriers (NLC) in cosmetic and dermatological preparations. *Advanced Drug Delivery Reviews* 54: S131-S155.

Ni, S., Sun, R., Zhao, G. & Xia, Q. 2014. Quercetin loaded nanostructured lipid carrier for food fortification: Preparation, characterization and *in vitro* study. *Journal of Food Process Engineering* 38(1): 93-106.

Sakamula, R., Yata, T. & Wachiryah, T-A. 2021. Effects of alpha-mangostin encapsulated in nanostructured lipid carriers in mice with cerebral ischemia reperfusion injury. *Sains Malaysiana* 50(7): 2007-2015

Sarheed, O., Dibi, M. & Ramesh, K.V.R.N.S. 2020. Studies on the effect of oil and surfactant on the formation of alginate-based O/W lidocaine nanocarriers using nanoemulsion template. *Pharmaceutics* 12(12): 1223.

Severino, P., Pinho, S.C., Souto, E.B. & Santana, M.H.A. 2011. Polymorphism, crystallinity and hydrophilic-lipophilic balance of stearic acid and stearic acid-capric/caprylic triglyceride matrices for production of stable nanoparticles. *Colloids and Surfaces B: Biointerfaces* 86(1): 125-130.

Shirodkar, R.K., Kumar, L., Mutalik, S. & Lewis, S. 2019. Solid lipid nanoparticles and nanostructured lipid carriers: Emerging lipid based drug delivery systems. *Pharmaceutical Chemistry Journal* 53(5): 440-453.

Souto, E.B. & Müller, R.H. 2006. Investigation of the factors influencing the incorporation of clotrimazole in SLN and NLC prepared by hot high-pressure homogenization. *Journal of Microencapsulation* 23(4): 377-388.

Subramaniam, B., Siddik, Z.H. & Nagoor, N.H. 2020. Optimization of nanostructured lipid carriers: Understanding the types, designs, and parameters in the process of formulations. *Journal of Nanoparticle Research* 22(6): 1-29.

Teo, Y.Y., Misran, M., Low, K.H. & Zain, S.M. 2011. Effect of unsaturation on the stability of C18 polyunsaturated fatty acids vesicles suspension in aqueous solution. *Bulletin of the Korean Chemical Society* 32(1): 59-64

Vieira, R., Severino, P., Nalone, L.A., Souto, S.B., Silva, A.M., Lucarini, M., Durazzo, A., Santini, A. & Souto, E.B. 2020. Sucupira oil-loaded nanostructured lipid carriers (NLC): Lipid screening, factorial design, release profile, and cytotoxicity. *Molecules* 25(3): 685.

Yew, H.C. & Misran, M. 2019. Progress in drug discovery & biomedical science characterization of fatty acid based nanostructured lipid carrier (NLC) and their sustained release properties. *Progress in Drug Discovery & Biomedical Science* 2(1): 1-7.

Zhang, N., Liu, C., Jin, L., Zhang, R., Siebert, H.C., Wang, Z., Prakash, S., Yin, X., Li, J., Hou, D. & Sun, B. 2020. Influence of long-chain/medium-chain triglycerides and whey protein/tween 80 ratio on the stability of phosphatidylserine emulsions (O/W). *ACS Omega* 5(14): 7792-7801.

*Corresponding author; email: misni@um.edu.my